JOURNAL OF MATERIALS SCIENCE 31 (1996) 3481–3486

Sliding wear of Al_2O_{3P}/6061 Al composite

S. J. LIN
Department of Materials Science and Engineering, Tsing Hua University, Hsinchu, Taiwan
C. A. LIN, G. A. WU, J. L. HORNG
Materials Research Laboratories, ITRI, Hsinchu, Taiwan

The mild sliding wear behaviour of a 15 vol % Al_2O_{3p}/6061 Al composite has been investigated by using a pin-on-disc reciprocating sliding machine. The composite has been shown to exhibit an excellent wear resistance as compared to the unreinforced matrix alloy. The wear rate of the composite under dry wear conditions with a 12N load is approximately one tenth of that in the 6061 aluminium alloy. The wear rate of the composite under lubrication with 15W/40 gear oil under a 100N load is only one thousandth of that in the 6061 aluminium alloy.

The dry wear resistance of an over-aged sample is shown here to be better than a peak aged or under-aged sample when the composite was aged at 160 °C. The coefficient of friction of the composite was approximately 0.5–0.6 under dry conditions and 0.07 in lubricated wear experiments.

In the initial stage, the worn surface of the composite under dry conditions is primarily composed of ploughed grooves and ductile tear. The composite makes a conducting contact with the steel pin. The worn surface is composed of compacted powder and the contact potential gradually increases when the period of the wear experiment goes beyond 2 h.

1. Introduction

Ceramic particle reinforced aluminium metal matrix composites have advantages over aluminium alloys in strength, stiffness and wear resistance. Their development has received increased emphasis in the last decade [1]. Some commercial products for Al_2O_3 or SiC particle reinforced aluminium alloy composites exist which have been used in many application areas [2, 3]. Investigations on the wear behaviour of particle reinforced aluminium alloy composites have been reported for in the graphite/Al composite [4, 5] and the SiC_w/Al composite [6, 7]. The wear properties of the commercial product Duralcan have, however, been seldom reported [8]. A type of Duralcan, i.e. 15 vol % Al_2O_{3p}/6061 Al composite has thus been chosen for study here. The effect of ageing treatments on the wear property is also investigated. The wear behaviour of the matrix 6061 Al was also studied to enable comparison with the composite.

2. Experimental procedure

The ingot of 15 vol % Al_2O_{3p}/6061 Al composite was purchased from Alcan Co. and was extruded at 500 °C with a 5: 1 extrusion ratio. The ingot was formed into a bar shape with a 30 mm diameter. The wear specimen, a disc plate, was cut from the bar and then solution treatment was performed at 530 °C for 2 h. The specimen was aged (after quenching) at 160 °C or 175 °C. Four samples with different ageing conditions were produced these were, 160 °C under-aged, 160 °C peak-aged, 160 °C over-aged and 175 °C peak-aged. Their corresponding hardness values were HRB 66, 72, 66 and 69, respectively. The 6061 Al was aged at 175 °C and achieved a peak-aged condition. Its hardness was HRB 63.

The high frequency wear test machine manufactured by Cameron Plint Company was used in these studies. It was a pin-on-disc type with a reciprocating sliding wear test facility. The test details are shown in Fig. 1. The composite or 6061 Al samples to be tested

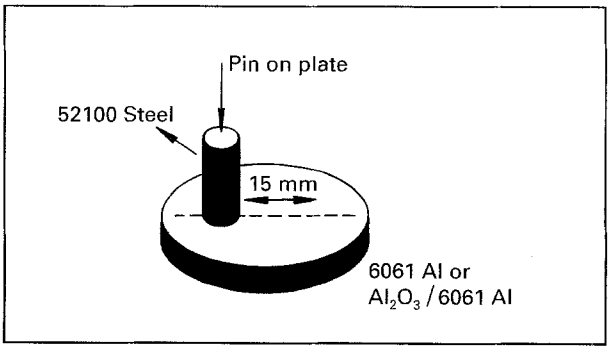

Figure 1 Schematic diagram of pin-on-disc, reciprocating sliding wear test.

0022–2461

became the disc plate, and were 30 mm in diameter and 4 mm in thickness. A 52100 steel pin with a HRC 60 hardness was chosen as the counterpart with dimensions of 6 mm diameter and 20 mm length.

Before the wear test, the samples were polished with 6 μm and 3 μm diamond paste and the mass was weighed as being 0.01 mg. The wear load was respectively 12 N and 100 N for dry wear experiments and lubricated wear experiments (with 15W/40 gear oil) respectively. The sliding velocity was 0.15 ms^{-1} and the maximum sliding distance was 4320 m.

3. Results and Discussion

3.1. The effect of ageing conditions on the weight loss

The effect of the ageing condition at 160 °C on the weight loss in a dry sliding wear test is shown in Fig. 2. The smallest weight loss was found for the over-aged sample. The hardness of the under-aged sample is the same as the over-aged sample, i.e. HRB 66. The wear resistance of the over-aged sample is obviously better than that of the under-aged sample. The wear behaviour can therefore be influenced by ageing conditions. The abrasive wear in SiC_p/Al–Zn–Mg composites were studied by Lin *et al.* [9] and similar results were obtained. Comparable results were also attained by Lee *et al.* [10].

3.2. The variation of wear rate

The wear rate of a specimen is defined as the ratio of weight loss to the total sliding distance. The dry wear rates for different specimens are shown in Table I. The wear rate of the 15 vol % Al_2O_{3p}/6061 Al composite peak-aged at 175 °C is slightly higher than that of the 160 °C-aged specimens irrespective of ageing condition. Approximately, an order of magnitude higher wear rate exists for the 6061 Al as compared to the composite. The wear rate of the steel counterpart is, however, an order of magnitude lower than that of the composite.

Some lubricated wear data are also shown in Table I. The wear rate of the specimens under lubricated conditions is much lower than the dry wear rate. This is true even though the load of the lubricated wear (100N) is much higher than that of the dry wear condition (12N). The wear resistance of the composite can be seen here to be outstanding under lubricated conditions when compared to the wear resistance of the 6061 Al under dry and lubricated conditions. The lubricated wear rate of the composite is only one thousandth of the 6061 Al.

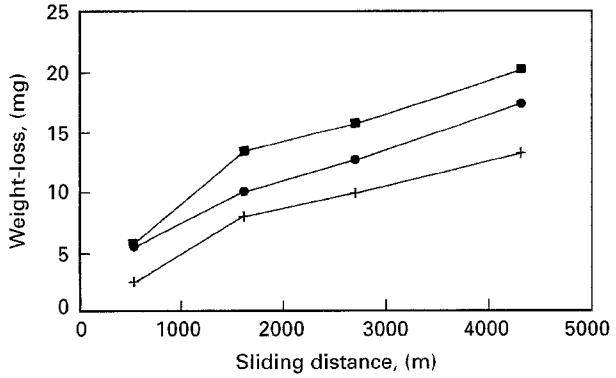

Figure 2 The weight loss of the composite aged at 160 °C , under dry sliding wear conditions. The samples were (■) under-aged, (●) peak-aged and (+) over-aged.

TABLE I Wear Rate for different specimens

Specimen	Dry wear rate $\times 10^{-12}\ m^3\ m^{-1}$	Lubricated wear rate $\times 10^{-15}\ m^3\ m^{-1}$
Composite		
160 °C, under-aged	1.85	—
160 °C, peak-aged	1.62	2.20
160 °C, over-aged	1.34	—
175 °C, peak-aged	0.192	2.40
6061 Al		
175 °C, peak-aged	9.20	2.40×10^3
Steel pin against composite	0.14	7.00

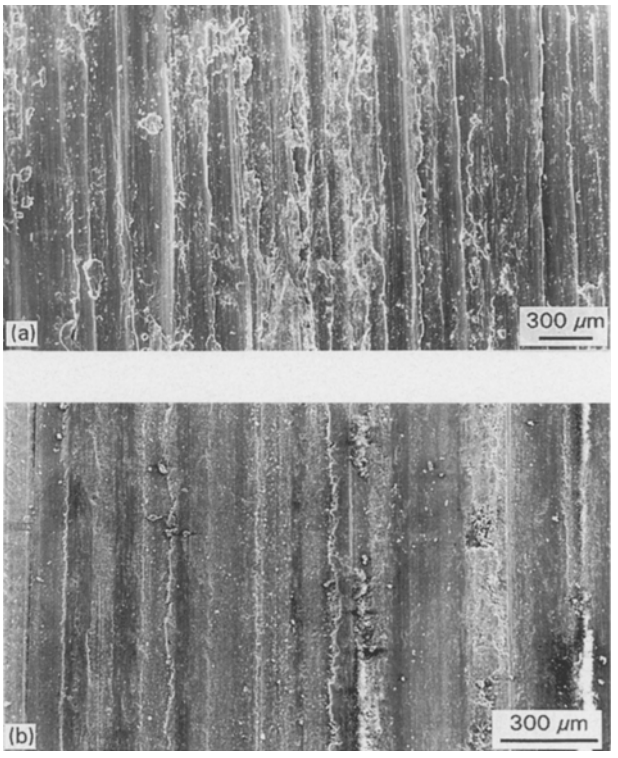

Figure 3 Typical microstructure of worn surface under dry sliding wear (a) 6061 Al, 175 °C peak-aged, (b) composite, 160 °C peak-aged.

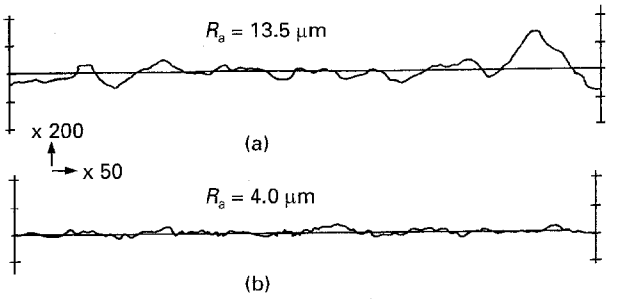

Figure 4 Typical roughness of worn surface under dry sliding wear (a) 6061 Al, 175 °C peak-aged, (b) composite, 160 °C peak-aged.

From the above results, it is obvious that the wear resistance of the 15 vol % Al_2O_{3p}/6061 Al composite is superior to that of the 6061 aluminium alloy, especially under lubricated conditions. The typical worn surface structures of the composite and the 6061 Al alloy are shown in Fig. 3. Many scraped wear scores exist in the worn surface. The major wear mechanism is indicated by this to be abrasive wear. The rubbed scores of the aluminium alloy are heavier than that of the composite, as is shown in Fig. 3. This phenomenon can be verified by the roughness measurement. Fig. 4 shows the roughness index R_a of the Al-alloy to be 13.5 μm, whilst being only approximately 4 μm in the composite. The larger roughness values mean that more material was rubbed out resulting in a higher abrasion rate for the Al-alloy than for the composite.

The wear scores in the lubricated wear condition are finer than in the dry wear condition. The roughness is approximately 8 μm for the Al-alloy and 0.3 μm for the composite. These data explains why the wear rate is lower under lubricated conditions than under dry conditions and why the wear resistance of the composite under lubricated conditions is so outstanding.

3.3. The variation of the coefficient of friction and contact potential

The typical variation of the coefficient of friction and contact potential during the sliding wear process are shown in Fig. 5. The coefficient of friction is approximately 0.9 for the Al-alloy and 0.5–0.6 for the composite. The variation of the contact potential is different between the Al-alloy and the composite. In the 6061 Al, a conducting contact is formed with the steel-pin counterpart during the wear process. In the composite, a conducting contact condition only exists during the initial stage of the wear process. However, the contact potential fluctuated between 0 and 35 mV after two hours (corresponding to a sliding distance of 1080 m). This implies the existence of an interface which results in poor conductivity between the steel pin and the composite. This interface is unstable and makes the contact potential unsteady.

The coefficient of friction decreases in the lubricated wear experiments to approximately 0.35 for the 6061 Al alloy and 0.07 for the composite, as shown in Fig. 6. The contact potential gradually increases to 25 mV for the Al-alloy and 43 mV (insulating condition) for the composite.

Two different variations can be found when comparing the lubricated and dry sliding wear conditions. Firstly, the coefficient of friction decreases and the contact potential increases when the wear test is conducted under the lubricated conditions. Secondly, more steady data exist under the lubricated condition, especially for the coefficient of friction. These phenomena must have resulted from the entrance of the gear oil into the interface between the pin and plate.

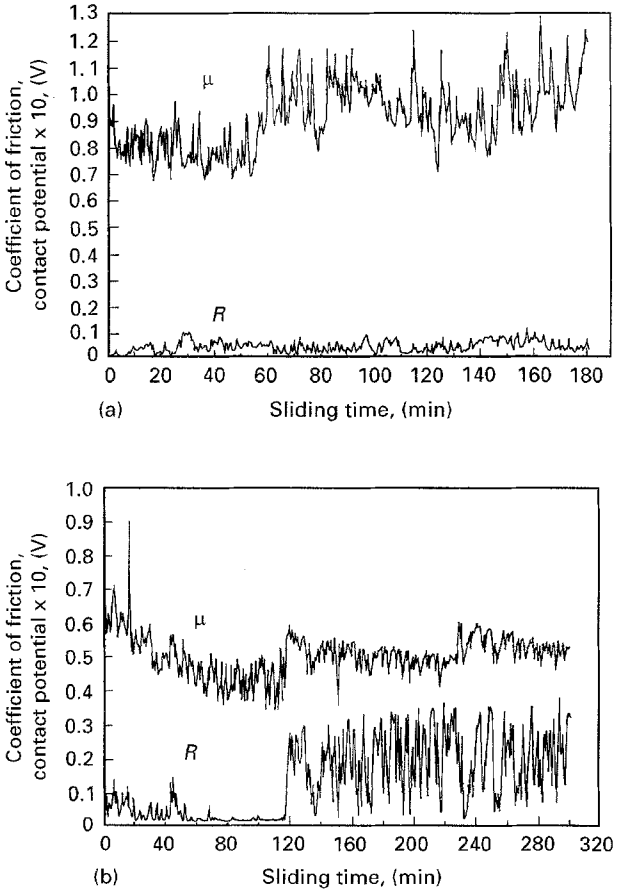

Figure 5 The variation of coefficient of friction (μ) and contact potential (R) during dry sliding wear process (a) 6061 Al, 175 °C peak-aged, (b) composite, 160 °C peak-aged.

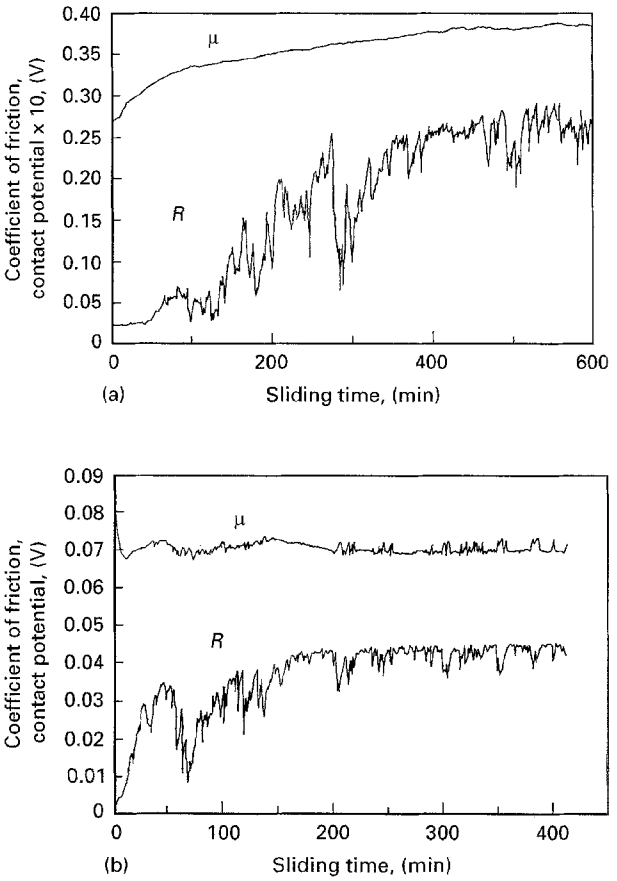

Figure 6 The variation of coefficient of friction (μ) and contact potential (R) during lubricated sliding wear process (a) 6061 Al, 175 °C peak-aged, (b) composite, 160 °C peak-aged.

3.4. The development of the surface microstructures of the composite during sliding wear

Table II shows the wear rate and roughness for specimens of the 175 °C peak-aged condition composite for different sliding times. The wear rate and roughness gradually decreased as the sliding time increased. The larger surface roughness is thought to result in a higher wear rate for the initial stage of wear. When the sliding time is longer, the roughness of the worn surface gradually decreases and the wear rate is lower.

The microstructures of the worn surface of the peak-aged composite for different sliding times are shown in Fig. 7. The left hand side of each micrograph shows the secondary electron image (SEI) image and the right hand side micrograph shows the back scattering electron image (BEI) image. The BEI images show the density of surface material more clearly than the SEI images. A comparison of the wear scores seen in the micrographs shows that they become finer and finer as the sliding time increases. At the initial stage of wear (sliding time less than 2 h) the major part of the worn surface was composed of ploughed grooves and ductile tears which were flattened by the subsequent sliding of the steel pin. This is shown in Fig. 7a. A higher magnification photo is shown in Fig. 8a. Some cracking can also be observed in the tear edge. These tear edges may be fractured, thereby becoming detached and forming debris or they may be flattened again by subsequent sliding.

TABLE II Wear rate and roughness of worn surface of the composite (175 °C, peak-aged) under dry condition for different sliding times.

Sliding time	Wear rate, $\times 10^{-12}\ m^3\ m^{-1}$	Roughness, R_a μm
38 min	3.36	5.4
2 h	3.04	5.2
3 h	2.72	3.4
8 h	1.92	2.9

The quantity of fractured debris continuously increased once the sliding time exceeded 2 h. The debris were compacted and smoothed between the composite plate and the steel pin. The worn surface was composed of compacting powder and a smoothing area. These phenomena are shown in Fig. 7(c, d). A typical worn surface of such condition with higher magnification is shown in Fig. 8b.

The sliding time of Fig. 7b is 2 h which corresponds to its transition stage. The worn surface is composed of ploughed areas and compacted powder.

The composite was in direct contact with the steel pin during the initial stage of wear (since the interfacial layer had not fully formed). The contact potential was near zero, as shown in Fig. 5b. An interfacial layer composed of compacted powder with a lower conductivity was established when the sliding time increased. The contact potential was then significantly increased. The observed large fluctuations in the contact potential was attributed to the different

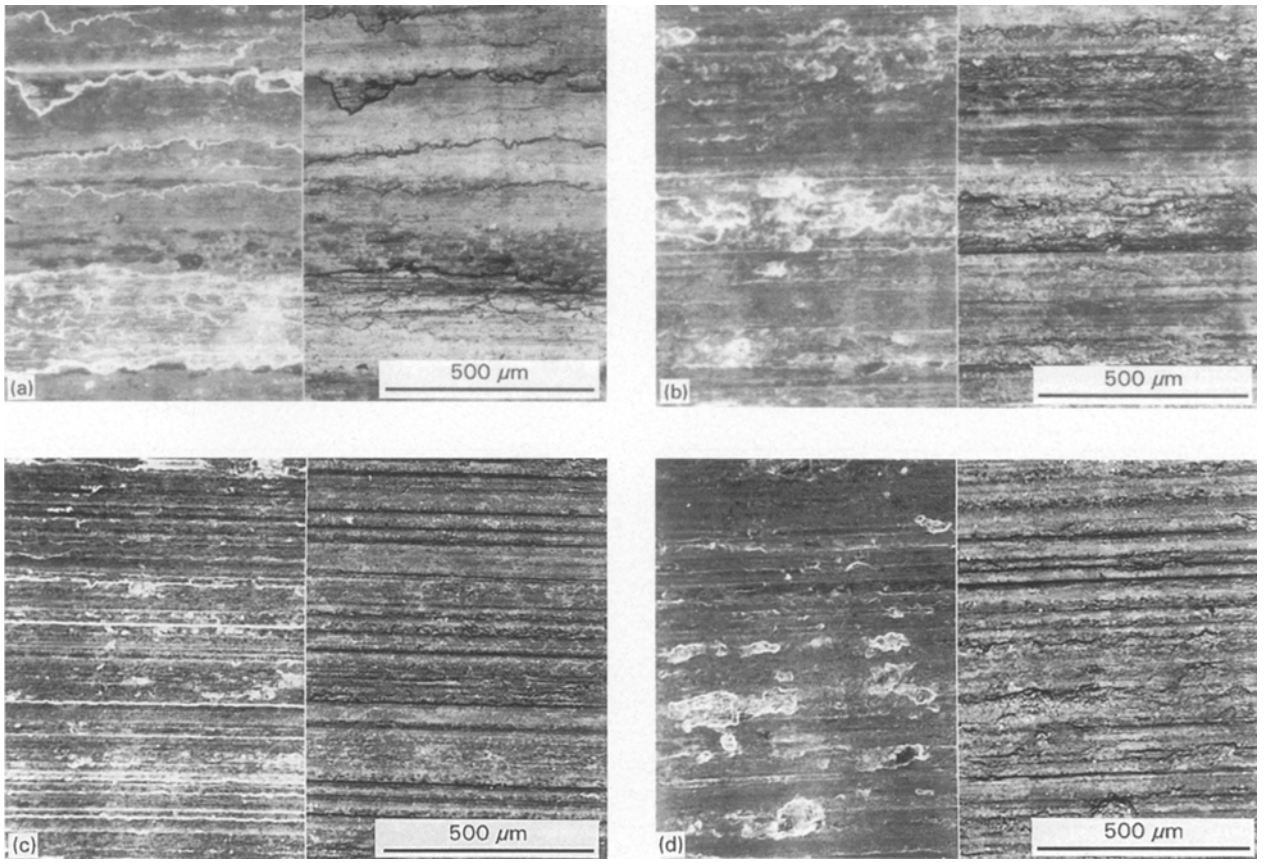

Figure 7 Microstructure of worn surface of the composite for different sliding times under dry conditions. Left: SEI image; right: BEI image. (a) 20 min, (b) 2 h, (c) 3 h, (d) 8 h.

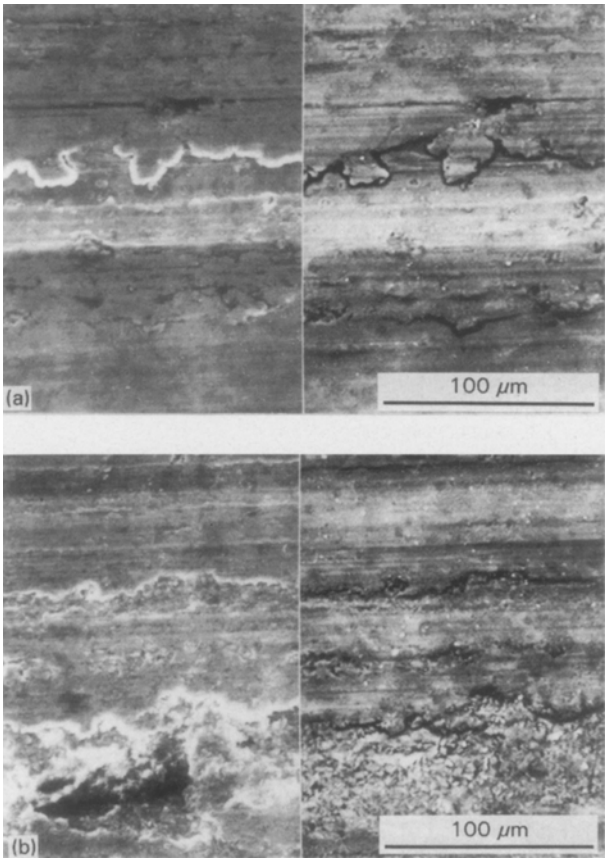

Figure 8 Microstructure of worn surface of the composite for different sliding times under dry conditions. Left: SEI image; right: BEI image. (a) 38 min, (b) 8 h.

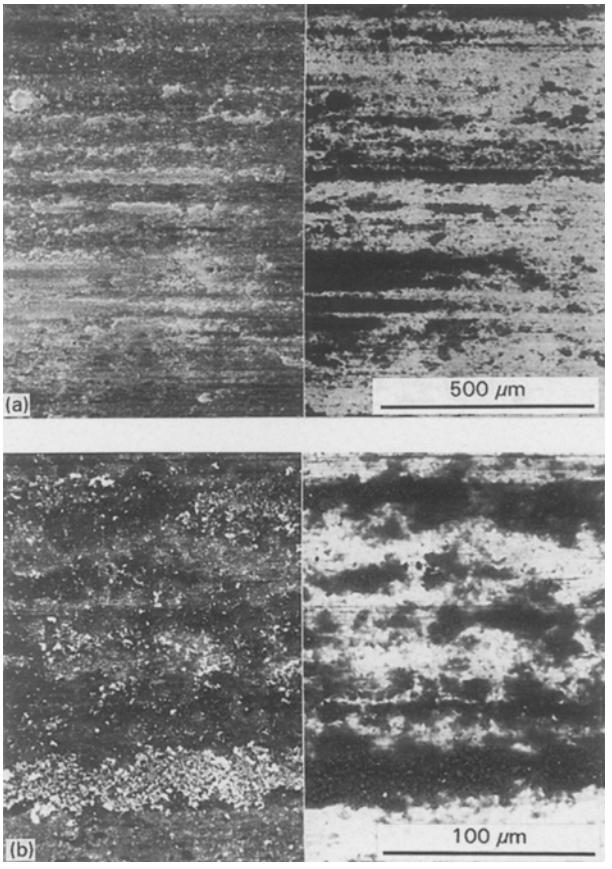

Figure 9 Microstructure of worn surface of the counterpart steel pin which wore with the composite under dry sliding condition. Left: SEI image, right: BEI image. (a) lower magnification, (× 80) (b) higher magnification. (× 400)

degree of powder compacting which was varying for each cycle of wear. These phenomena are also shown in Fig. 5b.

Many wear scars which make the worn surface rougher can be seen in Fig. 7. The production of wear scars may be due to the transfer of the composite material into the steel pin surface. The worn surface of the steel pin is shown in Fig. 9. Many dark areas exist which correspond to lighter elements in a BEI image. Thus composite debris is indicated by this micrograph to have adhered onto the steel pin surface, i.e. a transfer phenomenon.

Back-transfer is observed to have occurred from the steel pin to the composite surface in some areas of the worn surface of the composite, as is shown in Fig. 10. These are bright areas in the BEI image which indicate a heavier element, such as Fe has been retained in the worn surface of the composite. The micrograph also shows the existence of many transverse cracks in the back-transfer material.

The superior wear resistance of the composite is a result of the presence of Al_2O_3 particles. This can be seen clearly under the lubricated conditions which showed the least wear. A BEI image of a worn surface of the composite under lubricated condition is shown in Fig. 11. The dark areas are Al_2O_3 particles and the bright spots are iron-rich particles. Besides fine iron-rich particles dispersed in the worn surface, many larger iron-rich particles beneath Al_2O_3 particles

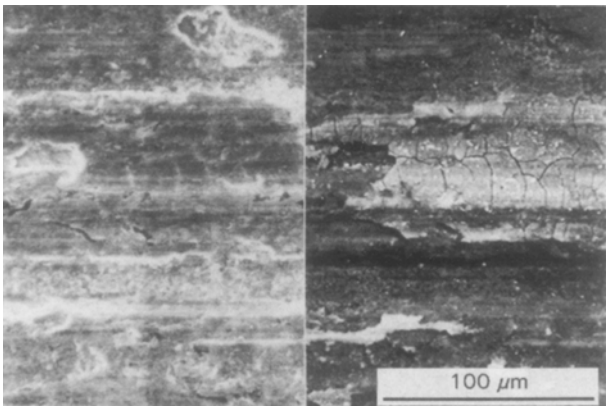

Figure 10 Microstructure of worn surface of the composite after 3 h sliding under dry condition. Left: SEI image; right: BEI image.

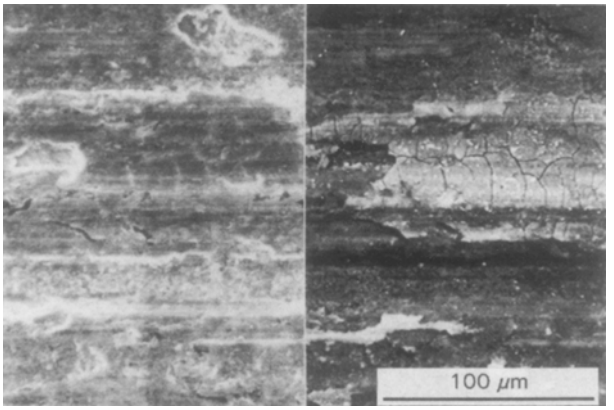

Figure 11 BEI image of worn surface of the composite after 8 h sliding under lubricated condition.

are also observed. These larger iron-rich particles are scraped from the steel pin by the Al_2O_3 particle. Many blurred dark areas are seen to exist in the BEI image when checking Fig. 8 in detail. This indicates that Al_2O_3 particles have survived in the worn surface during all periods of the sliding wear process and results in the superior wear resistance of the composite.

4. Conclusions

1. The dry wear resistance of an over-aged sample has been shown to be better than a peak-aged sample when the 15 vol % Al_2O_{3p}/6061 Al composite was aged at 160 °C .

2. The wear resistance of the composite is superior to the 6061 Al matrix alloy, especially under lubricated conditions. The wear rate of the composite under lubricated conditions is only about one thousandth of that of the 6061 aluminium alloy.

3. The coefficients of friction for the composite are 0.5–0.6 under dry sliding wear and 0.07 under lubricated sliding wear.

4. In the initial stage, the worn surface of the composite under dry wear was primarily composed of ploughed grooves and ductile tears. The composite was in direct conducting contact with the steel pin. When the sliding period of dry wear was longer than 2 h, the worn surface was composed of a compacted powder interface with a lower conductivity and the contact potential significantly increased.

References

1. P. K. ROHATGI, R. ASTHANA and S. DAS, *Inter. Met. Rev.* **31** (1986) 115.
2. P. K. ROHATGI, *JOM* (1991) 10.
3. DURALCAN Composites, Mechanical and Physical Property Data, Alcan, Feb. 26, 1990.
4. P. K. ROHATGI, Y. LIU, M. LIN and T. L. BARR, *Mat. Sci. Eng.* **A123** (1990) 213.
5. P. K. ROHATGI, Y. LIU and T. L. BARR, *Met. Trans. A* **22A** (1991) 1435.
6. L. CAO, Y. WANG and C. K. YAO, *Wear* **140** (1990) 273.
7. A. WANG and H. J. RACK, *Ibid.* **147** (1991) 355.
8. Y. S. CHIAO, F. M. PAN, C. A. LIN, J. L. HORNG and S. J. LIN, *Ibid.* **161** (1993) 155.
9. S.-J. LIN and K.-S. LIU, *Ibid.* **121** (1988) 1.
10. H. L. LEE, W. H. LU and S. L. I. CHAN, *Chinese J. Mater. Sci.* **24** (1992) 40.

Received 9 May 1995
and accepted 1 December 1995